JMEPEG (2017) 26:5079–5084
DOI: 10.1007/s11665-017-2932-z

1059-9495/$19.00

Effect of Cryogenic Treatment on Microstructure and Mechanical Properties of 0Cr12Mn5Ni4Mo3Al Steel

Xue Bai, Linbin Zheng, Jinyan Cui, Sujun Wu, Ruokang Song, Di Xie, Dawei Wang, and Haisheng Li

(Submitted November 10, 2016; in revised form May 24, 2017; published online September 20, 2017)

This paper systematically investigated the effect of cryogenic temperature and soaking time on the 0Cr12Mn5Ni4Mo3Al steel. Microstructure observation and mechanical tests were performed on the specimens by scanning electron microscopy, x-ray diffraction, Vickers hardness tests and tensile tests. Cryogenic treatments were carried out at different temperatures of −73, −120, −160 and −196 °C for a given soaking time of 4 h and at a specific temperature of −73 °C for different soaking time of 8, 12, 21 and 32 h, followed by the subsequent tempering treatment. The results showed that the volume fraction of martensite in this steel has significantly increased and the size of martensite lath has decreased after cryogenic treatment, which leads to the improvement of the mechanical properties of the steel. The cryogenic treatment affected the microstructure by promoting the transformation of retained austenite to martensite and the formation of reversed austenite in the steel. The optimal hardness and strength of this steel were obtained by cryogenic treatment at −73 °C for 8 h. It has been found that the soaking time is a critical parameter for the mechanical properties of 0Cr12Mn5Ni4Mo3Al steel. When the cryogenic temperature is lower than −73 °C, there is no further improvement of the mechanical properties.

Keywords 0Cr12Mn5Ni4Mo3Al, cryogenic treatment, mechanical properties, microstructure

1. Introduction

Cryogenic treatment is a process of chilling down the material to far below room temperature. The process is a supplementary of traditional treatment, which has just been developed for a few decades (Ref 1-4). Cryogenic treatment, as an economical, simple, environmentally friendly method, can improve the mechanical properties of materials by optimizing microstructure, so that many researchers focus on the investigation of the beneficial effect of cryogenic treatment on steels (Ref 5-8).

0Cr12Mn5Ni4Mo3Al steel is the precipitation hardening stainless steel which has high strength, good ductility, well fracture toughness and excellent corrosion resistance. Therefore, the steel has been widely used as airplane wing leading edge, flare-less pipe joints, elastic component (Ref 9-13). The excellent comprehensive property of the 0Cr12Mn5Ni4Mo3Al steel can be attributed to its high alloying elements additions. It is well known that Cr and Ni can significantly improve the corrosion resistance, strength and hardness of the steel while Mn efficiently improves the strength and minimizes the bad influence of sulfur. The addition of the Mo increases tempering resistance of the steel, while Al can generate NiAl and Ni_3Al precipitates to improve the strength. At the same time, the elements of C, Cr, Ni, Mo can promote the Ms (martensite start point, which is slightly below 0 °C) to drop, which can indirectly affect the strength and toughness (Ref 14).

At present, solution and aging treatments have been well developed to improve the mechanical properties of 0Cr12Mn5Ni4Mo3Al steel. Though Cao (Ref 10) studied the effect of different cryogenic temperatures (0, −20, −40, −60 and −78 °C) on the properties of 0Cr12Mn5Ni4Mo3Al, the lower temperature which might affect the properties of steel has not been investigated (Ref 15). Moreover, the effect of the soaking time on properties of the steel was also neglected. Hence, this paper adopted a treatment on the steel with a series of different cryogenic temperature and soaking time, and focused on the effects of different cryogenic treatment parameters on the microstructure evolution and mechanical properties at room temperature. The results can facilitate the application of cryogenic treatment on 0Cr12Mn5Ni4Mo3Al steel in practice.

2. Materials and Methods

2.1 Material and Treatment

The raw material (0Cr12Mn5Ni4Mo3Al steel) after solution treatment was provided by Chengdu aircraft industrial (Group) Co., Ltd. The parameter of solution treatment was 1050 °C for 0.5 h, then the material was quenched in oil. The actual chemical composition of the steel is shown in Table 1. The cryogenic treatment was conducted using the SLX series program-controlled cryogenic system and YDZ200 liquid nitrogen container, followed with tempering treatment. The steel was divided into nine groups for the different cryogenic treatment at the same cooling rate of 3 °C/min. After the cryogenic treatment, tempering treatment was conducted on all of the nine group specimens. The specimens were heated to 520 °C with a heating rate of 10 °C/min, held for 12 h at

Xue Bai, Jinyan Cui, Sujun Wu, Ruokang Song, and **Di Xie**, School of Materials Science and Engineering, Beihang University, Beijing 100191, People's Republic of China; and Beijing Key Laboratory of Advanced Nuclear Materials and Physics, Beihang University, Beijing 100191, People's Republic of China; **Linbin Zheng, Dawei Wang,** and **Haisheng Li**, Chengdu Aircraft Industrial (Group) Co., Ltd., Chengdu 610092, China. Contact e-mail: wusj@buaa.edu.cn.

520 °C, and then air-cooled to room temperature. The detailed treatment processes are shown in Table 2. The dimensions of the used specimens are 10 mm × 10 mm × 1 mm.

2.2 Microstructure Observation

Field emission scanning electron microscopy (SEM) (QUANTA 250 FEG) and the x-ray diffraction (XRD) (D/Max-2500) were used for phase and microstructure analysis of this 0Cr12Mn5Ni4Mo3Al steel. The specimens for SEM observation were etched using the solution consisting of 5 g $FeCl_3$, 10 mL HCl and 50 mL H_2O. The working voltage and the working electric current for XRD analysis were 40 kV and 200 mA, respectively. In order to obtain the detailed information of the nano-precipitates, the high-resolution transmission electron microscopy (HRTEM, JEOL JEM 2100) has been employed to study them.

2.3 Mechanical Properties Tests

The tensile tests based on GB/T228.1 (Ref 16) were conducted using Instron 8801 hydraulic servo device equipped with a 50kN load cell. All tests were performed at room temperature with a displacement rate of 0.5 mm/min. Hardness was measured using a Vickers hardness tester FM-800 at a load of 0.2 kgf for 15 s. The reported harness measurements are an average of at least five measurements taken on the sample.

3. Results and Discussion

3.1 Microstructure and Phase Analysis

The SEM micrograph of the specimen C0 shown in Fig. 1(a) indicates that the steel without cryogenic treatment consists of lath martensite, austenite and precipitates, which has been confirmed by XRD results in Fig. 2. According to previous investigations (Ref 9-11), these precipitates are mainly NiAl phases (little white point as indicated by arrows in Fig. 1), and the austenite consists of retained austenite and reversed austenite. The microstructure of NiAl phase was observed under the HRTEM, as shown in Fig. 3. Figure 3(a) shows the microstructure of NiAl phase, and Fig. 3(b) is the high-resolution electron diffraction pattern of NiAl phase. Comparing with the specimen C0, it can be seen that the volume fraction of martensite in specimens after cryogenic treatment has significantly increased, as shown in Fig. 1(b)-(i). The XRD results in Fig. 2 show that the peaks of (111) in γphase disappear or greatly decrease in the cryogenic treated specimens, which means that the reduction of austenite phase and increase in martensite phase. The mass fractions of austenite and martensite can be calculated by K method (RIR method) (Ref 17). The precipitates content can be ignored compared with austenite and martensite. In addition, the densities of austenite and martensite are taken as equal to the value (7.9) of the pure iron. According to above, the volume fractions of austenite and martensite can be obtained from the following equations:

$$V_\gamma = \frac{I_\gamma}{I_\gamma + K_M^\gamma I_M} \quad \text{(Eq 1)}$$

$$V_\gamma + V_M = 1 \quad \text{(Eq 2)}$$

where V is volume fraction and K is the intensity of reference. K_M^γ (0.74) is the specific value of RIR_γ (7.98) and RIR_M (10.81), and I is integral intensity.

The volume fractions of austenite and martensite determined by XRD are shown in Fig. 4, from which it could be found that the volume fraction of martensite has increased about 8-15% in the cryogenic specimens while the volume fractions of austenite correspondingly decreased. The size of martensite laths can also be obtained by employing the MDI JADE 5.0 software to analyze the XRD data (Ref 18, 19). The analysis results are shown in Fig. 5, which reveals that martensite lath size has been decreased after cryogenic treatment. Figure 6 shows the morphology of the martensite lath, from which it could be found that the lath size is about 200 nm. Comparison between specimens (C1-C4) at different cryogenic treatment temperature with the same soaking time (4 h) shows that the martensite lath size is not sensitive to treatment temperature. There are only tiny distinctions in martensite lath size of specimens C1-C4, and specimen C1 has the finest martensite lath size. However, the martensite lath size of specimens (C1, C5-C8) treated with different cryogenic soaking time at the same treatment temperature (−73 °C) changes dramatically, and the finest martensite lath size is obtained in specimen C5. Furthermore, it can be seen from Fig. 3 that the volume fractions of austenite in specimen C5 is lowest for all specimens. As shown in Fig. 2 that the peaks intensity of martensite (α) of C5 are higher than other specimens. This indicates that the volume fraction of austenite in specimen C5 is lowest.

From the above discussion, the cryogenic treatment has a significant influence on the phase transformation in 0Cr12Mn5Ni4Mo3Al steel. Most of retained austenite has transformed into martensite during cryogenic treatment, which leads to the increment of martensite lath and reduction of retained austenite. The refined microstructure discussed above can be attributed to the change of martensite crystal lattice constant or super-refined carbide precipitates (Ref 2). Moreover, the volume differences between crystal lattices of the origin austenite and the produced martensite would cause the transformation stresses. The cooling process to cryogenic

Table 1 Chemical composition of 0Cr12Mn5Ni4Mo3Al steel in wt.%

C	Mn	Si	Cr	Ni	Mo	Al	S
0.07	4.72	0.42	11.87	4.43	3.06	0.99	0.021

Table 2 Different process techniques of specimens in nine groups

No.	Cryogenic treatment	Tempering treatment
C0	No cryogenic treatment	520 °C × 12 h
C1	−73 °C × 4 h	520 °C × 12 h
C2	−120 °C × 4 h	520 °C × 12 h
C3	−160 °C × 4 h	520 °C × 12 h
C4	−196 °C × 4 h	520 °C × 12 h
C5	−73 °C × 8 h	520 °C × 12 h
C6	−73 °C × 12 h	520 °C × 12 h
C7	−73 °C × 21 h	520 °C × 12 h
C8	−73 °C × 32 h	520 °C × 12 h

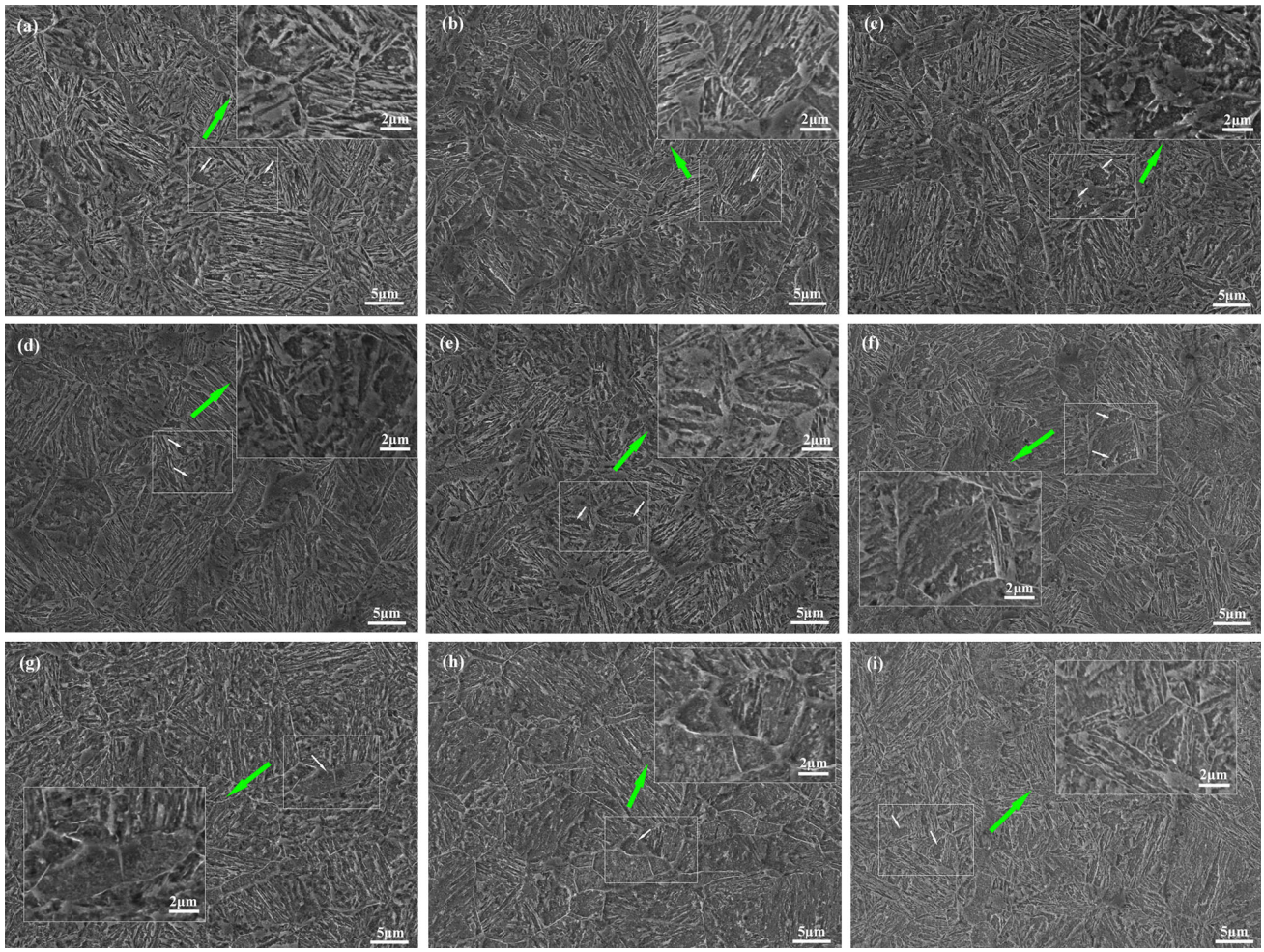

Fig. 1 Secondary electron images of nine specimens. (a) C0; (b) C1; (c) C2; (d) C3; (e) C4; (f) C5; (g) C6; (h) C7 and (i) C8

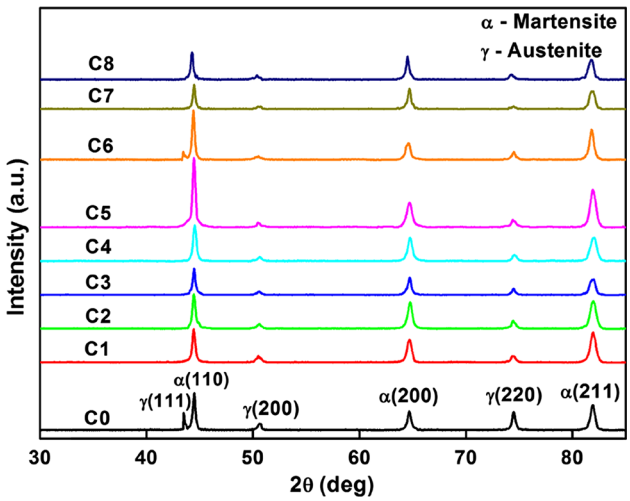

Fig. 2 XRD patterns in all specimens

temperature causes thermal contraction. The transformation stresses and thermal contraction would be the thermodynamic driving force during the cryogenic treatment, which makes carbon atoms hard to have long-range diffusion to redistribute, but easier to have short-range diffusion to form precipitates (carbides). The severe lattice distortion and high inner energy attribute to the microstructure refinement of the steel (Ref 6, 20).

3.2 Mechanical Properties and Optimized Cryogenic Parameters

The Vickers hardness results of specimens with different cryogenic temperature and different soaking time are shown in Fig. 7. Comparing the hardness of specimens C1-C4, it can be seen that hardness of specimens processed with same cryogenic soaking time of 4 h at different temperature is almost identical but a little bit higher than that of specimen C0. However, the hardness results of specimens (C1, C5-C8) treated at the same cryogenic temperature of −73 °C for different soaking time varies from each other. It can be concluded that the soaking time has a significant effect on the hardness of 0Cr12Mn5Ni4-MoAl steel while the cryogenic temperature shows a negligible effect. The specimen C5 possesses the highest hardness value, 447 HV, which is 15.8% higher compared with C0 sample. The variation trend of the hardness presented in Fig. 7 is similar with that of the austenite volume fraction illustrated in Fig. 4, which suggests that the specimen with the greater martensite proportion has higher hardness. Martensite is a carbon-super-

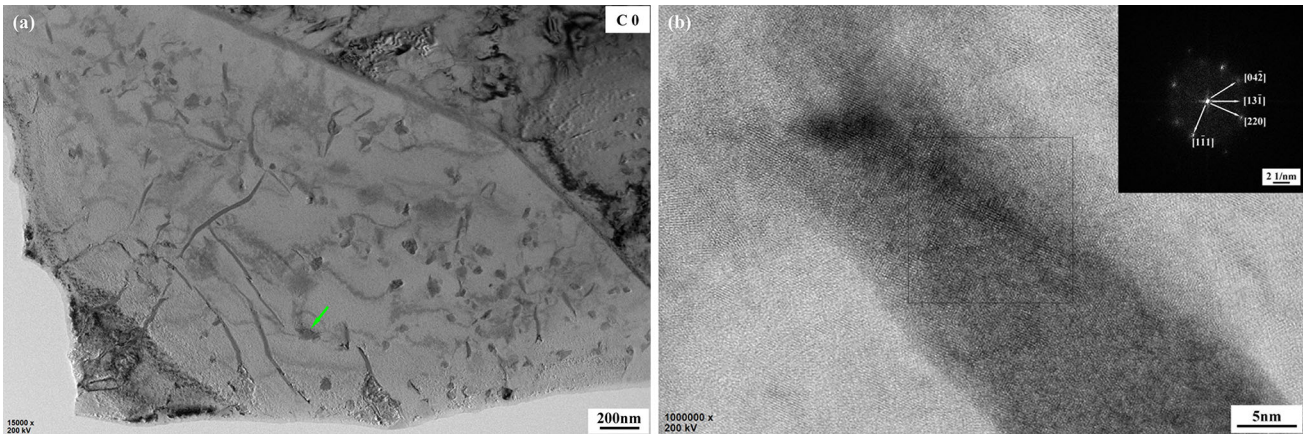

Fig. 3 The microstructure of NiAl phase observed under HRTEM, (a) microstructure of NiAl phase; (b) high-resolution electron diffraction pattern of NiAl phase

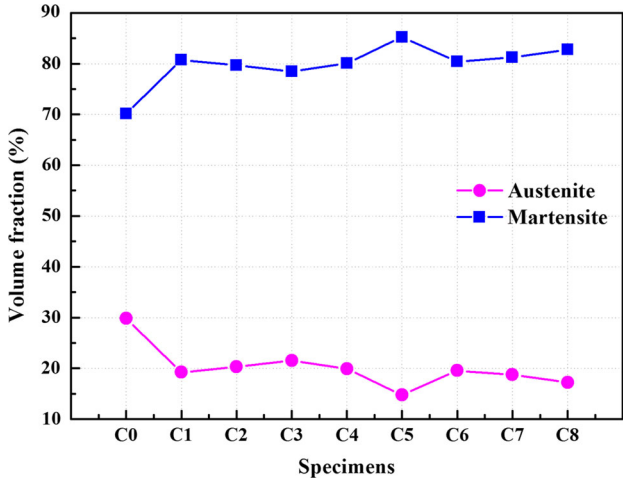

Fig. 4 Volume fractions of austenite and martensite in all specimens

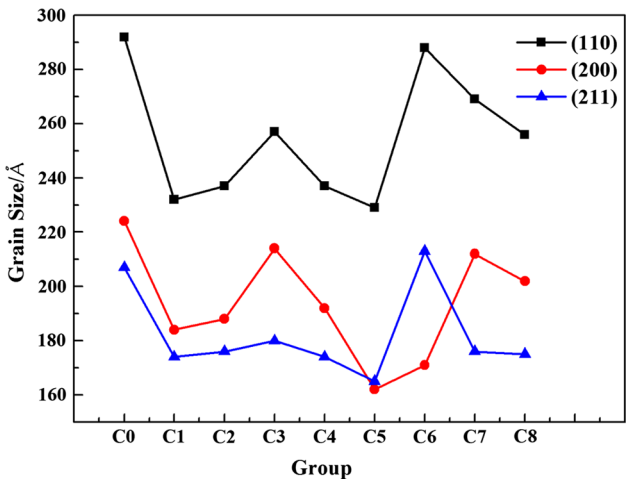

Fig. 5 Average size of the martensite laths in nine specimens

Fig. 6 The morphology of martensite lath of the 0Cr12Mn5Ni4-Mo3Al steel

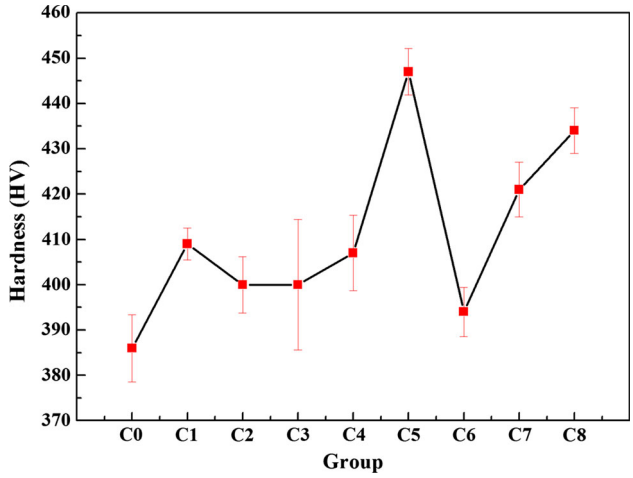

Fig. 7 Vickers hardness of specimens treated with different cryogenic parameters

saturated solid solution in which the lattice parameters for Fe and the vacancy concentration decrease at lower temperature, which increased the carbon supersaturation degree in the solid solution. All of these promote the precipitation of carbon and alloy atoms that not easily diffuse at low temperature, consequently, segregation of carbon and alloy atoms near dislocation lines occurred. This precipitation impedes the movement of dislocations, leading to an increase in the hardness after cryogenic treatment.

Tensile test results of the nine group specimens are shown in Fig. 6. Compared with specimen C0, the specimens after cryogenic process show superior tensile properties (σ_b improves ~ 22%, $\sigma_{0.2}$ improves ~ 50%) without severe loss in the elongation (δ). The comparison between specimens treated at different cryogenic temperature (Fig. 6) suggests that there is no distinct difference among the tensile properties of these specimens, which is consistent with the investigations of Guo et al. (Ref 9) and Cao (Ref 10). They have studied the effect of cryogenic temperature (0, −20, −40, −60, −78 °C) on mechanical properties of 0Cr12Mn5Ni4Mo3Al steel. The research results showed that the hardness and tensile properties improved by decreasing the cryogenic temperature, and the optimal cryogenic treatment parameters in their study was −78 °C for holding 4 h. They suggested that the transformation

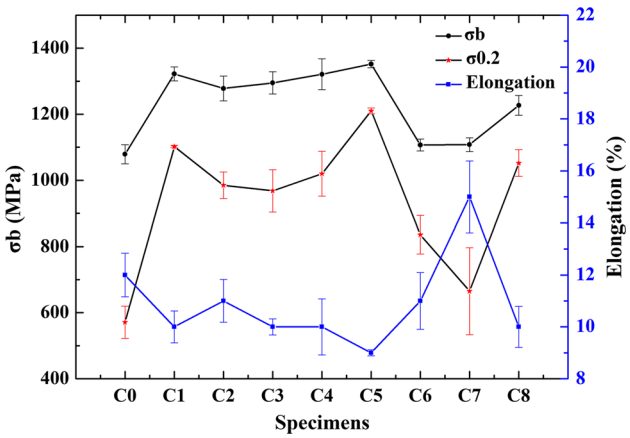

Fig. 8 Tensile test results of all specimens

of retained austenite to martensite during cryogenic treatment would be more sufficient at lower cryogenic temperature and the cryogenic temperature effect did not change anymore when the temperature was set lower than M_f (Martensite finishing point which is about −90 °C for the steel concerned). In addition, they believed that the soaking time has no effect on the 0Cr12Mn5Ni4Mo3Al steel due to the fast transformation of austenite to martensite during cryogenic treatment. However, the results in our study are different. The tensile strength of specimens (C1, C5-C8) changes with soaking time obviously (shown in Fig. 8). The group C5 possesses the highest tensile strength among them, but a little lowerδ than other groups. The mechanical properties of 0Cr12Mn5Ni4Mo3Al steel have a close relationship with the austenite proportion, consisting of retained austenite and reversed austenite. Many studies (Ref 17, 19-21) have indicated that cryogenic treatment can increase the phase change driving force and internal energy, which can promote the formation of reversed austenite during tempering treatment. The transformation of retained austenite to martensite is limited by austenite content, but the reversed austenite formation increases with the soaking time prolonging due to internal energy increase. The retained austenite transformation would prevail when the soaking time is set less than 8 h. Hence, the contradictory relationship between the transformation of retained austenite to martensite and the formation of reversed austenite along martensite lath might reach a balance point at −73 °C for 8 h, which explains the best strength performance of specimen C5 and the most evident change in martensite/austenite ratio in C5 specimen. Meanwhile, further optimization of the tempering technique is still needed to improve δ of C5.

As discussed above, there is no need to set cryogenic temperature lower than −73 °C for less cost. The optimal microstructure and mechanical properties are obtained for specimen C5. Therefore, the optimized cryogenic parameter is −73 °C for 8 h.

The tensile fracture surfaces of specimens C0 and C5 (Fig. 9) indicate the characteristics of ductile fracture of the two specimens. However, the dimples in specimen C5 are bigger and deeper than that in specimen C0, which is consistent with the tensile test data. In addition, the fine precipitated particles (indicated by circle in white) in the dimples in Fig. 9(b) can also improve the strength of the specimen.

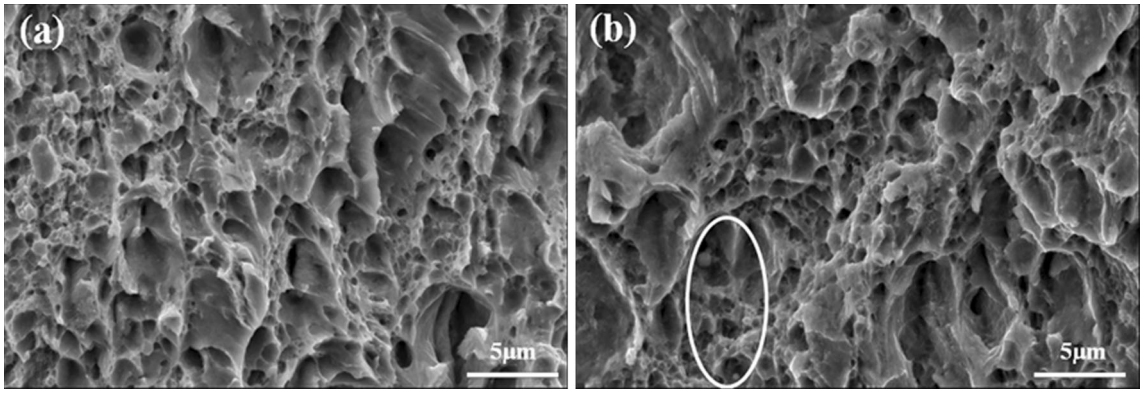

Fig. 9 Fracture surfaces of specimens (a) C0 and (b) C5

4. Conclusions

The effect of cryogenic treatment on microstructure and mechanical properties of 0Cr12Mn5Ni4Mo3Al was systematically investigated in this work. Several conclusions can be drawn as follows:

1. The martensite laths and austenite volume fraction decreased in specimens after cryogenic treatment. The optimal microstructure with finest martensite lath size and least austenite proportion is obtained in the specimen C5 at −73 °C for 8 h.
2. The soaking time has significant effect on the hardness and tensile properties of specimens. The strength and hardness of specimens treated at −73 °C increase with soaking time prolonging up to 8 h.
3. The optimal parameter of cryogenic treatment for 0Cr12Mn5Ni4Mo3Al steel is −73 °C for 8 h. Further research on cryogenic temperature lower than −73 °C for this steel is meaningless for the economic consideration. Effect of the soaking time is mainly attributed to the transformation of retained austenite to martensite and the formation of reversed austenite.

Acknowledgments

The authors wish to place their sincere thanks to the Chengdu aircraft industrial Co., Ltd., for financial support.

References

1. M. Araghchi, H. Mansouri, R. Vafaei, and Y. Guo, A Novel Cryogenic Treatment for Reduction of Residual Stresses in 2024 Aluminum Alloy, *Mater. Sci. Eng., A*, 2017, **689**, p 48–52
2. S.H. Li, K.Y. Zhao, K. Wang, and M.S. Yang, Microstructural Evolution and Thermal Stability After Aging of a Cobalt-Containing Martensitic Bearing Steel, *Mater. Charact.*, 2017, **124**, p 154–164
3. Y. Dong, X. Lin, and H. Xiao, Deep Cryogenic Treatment of High-Speed Steel and Its Mechanism, *Heat Treat. Met.*, 1998, **25**(3), p 55–59
4. R.F. Barron, Cryogenic Treatment of Metals to Improve Wear Resistance, *Cryogenics*, 1982, **22**(8), p 409–413
5. A. Akhbarizadeh, A. Shafyei, and M.A. Golozar, Effects of Cryogenic Treatment on Wear Behavior of D6 Tool Steel, *Mater. Des.*, 2009, **30**(8), p 3259–3264
6. A.I. Tyshchenko, W. Theisen, A. Oppenkowski, S. Siebert, O.N. Razumov, A.P. Skoblik, V.A. Sirosh, YuN Petrov, and V.G. Gavriljuk, Low-Temperature Martensitic Transformation and Deep Cryogenic Treatment of a Tool Steel, *Mater. Sci. Eng., A*, 2010, **527**(26), p 7027–7039
7. J.Y. Huang, Y.T. Zhu, X.Z. Liao, I.J. Beyerlein, M.A. Bourke, and T.E. Mitchell, Microstructure of Cryogenic Treated M2 Tool Steel, *Mater. Sci. Eng., A*, 2003, **339**(1-2), p 241–244
8. D. Senthilkumar, I. Rajendran, M. Pellizzari, and Juha Siiriainen, Influence of Shallow and Deep Cryogenic Treatment on the Residual State of Stress of 4140 Steel, *J. Mater. Process. Technol.*, 2011, **211**(3), p 396–401
9. Y.L. Guo, X.Q. Liu, X.M. Zhang, and J.T. Niu, Effect on Heat Treatment on Mechanical Properties of 0Cr12Mn5Ni4Mo3Al, *Acta Metall. Sin.*, 2004, **17**(2), p 118–121
10. S.L. Cao, *Research on Heat Treatment Process Parameters of 0Cr12Mn5Ni4Mo3Al)*, Harbin University of Science and Technology, Harbin, 2005 ((in Chinese))
11. F.M. Xue, F.G. Li, J. Li, and M. He, Strain Energy Density Method for Estimating Fracture Toughness from Indentation Test of 0Cr12Mn5Ni4Mo3Al Steel with Berkovich Indenter, *Theor. Appl. Fract. Mech.*, 2012, **61**, p 66–72
12. F.G. Li, F.M. Xue, W.J. Yu, and J.F. Li, Material Factors Analysis of the Cracking in 0Cr12Mn5Ni4Mo3Al Stainless Steel Pipe Sleeve on Aircraft Flare-Less Pipe Joints, *Adv. Mater. Res.*, 2011, **291–294**, p 1091–1094
13. H.R. Habibi-Bajguirani, The Effect of Aging Upon the Microstructure and Mechanical Properties of Type 15-5PH Stainless Steel, *Mater. Sci. Eng., A*, 2002, **338**(1–2), p 142–159
14. R.H. Yuan, J. Sun, G. Song, and J.F. Li, *Study on Milling Mechanism and Process Parameters Optimization of 69111 Stainless Steel*, Shandong University, Shandong, 2010 ((in Chinese))
15. H.H. Liu, J. Wang, B.L. Shen, H.S. Yang, S.J. Gao, and S.J. Huang, Effects of Deep Cryogenic Treatment on Property of 3Cr13Mo1V1. 5 High Chromium Cast Iron, *Mater. Des.*, 2007, **28**(3), p 1059–1064
16. GB/T228.1 (ISO 6892-1-2009 MOD), *Metallic Materials—Tensile Test—Part 1: Method of Test at Room Temperature*, Central Iron and Steel Research Institute, China, 2010, p 1–56
17. F.Z. Wang, *Analysis Techniques in Materials Science*, 1st ed., Beijing Institute of Technology, Beijing, 2016, p 73–92
18. N.A. Ozbek, A. Cicek, M. Gulesin, and O. Ozbek, Application of Deep Cryogenic Treatment to Uncoated Tungsten Carbide Inserts in the Turning of AISI, 304 Strainless Steel, *Metall. Mater. Trans. A*, 2016, **47**(12), p 6270–6280
19. J.W. Huang, MDI Jade Manual, 2006, p 13–22. http://www.docin.com/p-278032614.html
20. A. Zare, H. Mansouri, and S.R. Hosseini, Effect of Deep Cryogenic Treatment on the Microstructure and Mechanical Properties of HY-TUF Steel, *Metallogr. Microstruct. Anal.*, 2015, **4**(3), p 169–177
21. S.Q. Zheng, W. Jiang, X. Bai, S.H. Li, K.Y. Zhao, and X.K. Zhu, Effect of Deep Cryogenic Treatment on Formation of Reversed Austenite in Super Martensitic Stainless Steel, *J. Iron. Steel Res. Int.*, 2015, **22**(5), p 451–456